

Block copolymer as a template for electrically conductive nanocomposites

Dong Hyun Lee, Jeong Ah Chang and Jin Kon Kim*

Received 8th August 2006, Accepted 19th September 2006

First published as an Advance Article on the web 4th October 2006

DOI: 10.1039/b611456c

Electrically conductive nanocomposites were prepared by *in situ* polymerization of pyrrole in polystyrene-*block*-poly(*n*-butyl methacrylate) copolymer (PS-*b*-PnBMA) having lamellar microdomains, and characterized by using small angle X-ray scattering, transmission electron microscopy, and field emission scanning electron microscopy. For this purpose, the block copolymer film was immersed into a pyrrole–water mixture solution, followed by being immersed into FeCl₃–water solution. Since the pyrrole monomer was only partitioned into the PnBMA block, polypyrrole (Ppy) was only observed in PnBMA lamellar microdomains. The amount of Ppy in the block copolymer was varied by changing the immersion time of the block copolymer film into the pyrrole monomer solution. From the measured parallel and perpendicular conductivities of nanocomposites with various contents of Ppy by four-point and two-point probe techniques, respectively, the percolation threshold concentration of Ppy, above which nanocomposites behave as semiconductors, was very small (~ 2 wt%). The low value of the percolation threshold was due to the formation of electrical paths resulting from the lamellar microdomains of the PS-*b*-PnBMA.

Introduction

Although most organic compounds and polymers have been considered as insulators for a long time, some polymers exhibit electrical conductivity. Among these conductive polymers, polypyrrole (Ppy) has been extensively investigated because of its good environmental stability, high conductivity, and easy preparation either by chemical or by electrochemical polymerization.^{1–5} However, its applications have been restricted by several problems such as poor mechanical properties and poor processability.^{6–13} To overcome these drawbacks of Ppy, composites prepared by simply blending Ppy with various homopolymers were introduced.⁷ In this situation, macroscopically connected Ppy domains become electrical current paths. Because the theoretically predicted percolation limit is 16 vol% for a physical blend consisting of Ppy and polymers, the amount of Ppy added to conventional polymers should be over 16 vol% to exhibit sufficient conductivity because any macroscopically connected path does not exist below this concentration.¹⁴ Another method to prepare conductive composites is to use a specific polymer capable of favorably interacting with Ppy through a specific interaction like the hydrogen bond. The percolation threshold, above which electrical conductivity jumps dramatically, was reported to be ~ 7 vol% for a composite consisting of poly(bisphenol A carbonate) and Ppy, and it was ~ 10 vol% for another composite consisting of poly(vinyl methyl ketone) and Ppy.^{14,15} However, the electrical conductivities of these two composites were not high ($\sim 10^{-5}$ S cm⁻¹). Thus, an *in situ* polymerization of pyrrole monomer (py) inside the polymer

matrix was introduced to prepare composites with low percolation threshold and high conductivity. In this situation, the penetration of py into the polymer matrix is very important. To enhance the diffusion of py into the polymer, polymers should have functional groups to have specific interactions with py.^{12,13}

Recently, block copolymers have drawn considerable attention as new templates for *in situ* polymerization of conductive nanocomposites.^{6,7,13,16} Block copolymers exhibit well-ordered microdomains of 10–100 nm due to incompatibility and connectivity between two block segments.¹⁷ Once electrically conductive polymers are selectively incorporated into the microdomains of one block, these microdomains can be used as an electrical path. In this situation, the percolation threshold would be reduced greatly. Stankovic *et al.* prepared nanocomposites with a conductivity of 10^{-3} S cm⁻¹ by the exposure of polybutadiene-*block*-poly(2-vinylpyridine) copolymer to iodine vapor.⁶ Ishizu *et al.*⁷ showed that the nanocomposites prepared by the exposure of polystyrene-*block*-poly(2-vinylpyridine) copolymer (PS-*b*-P2VP) to methyl iodide vapor exhibited large differences between the parallel and perpendicular conductivities. But, both nanocomposites did not exhibit high conductivity. Furthermore, the stability of the conductivity of these nanocomposites was not good because doping agents were unstable under air. De Jesus *et al.*¹³ prepared nanocomposites by *in situ* polymerization of pyrrole in a sulfonated polystyrene-*block*-poly(ethylene-*alt*-propylene) copolymer (SPS-*b*-PEP) having lamellar microdomains (LAM). Due to the hydrophilicity of sulfonated polystyrene block segments, *in situ* polymerization of pyrrole monomer occurred only inside SPS microdomains. A relatively high parallel conductivity (10^{-3} – 10^{-1} S cm⁻¹) was achieved and the ratio of parallel to perpendicular conductivity was 1–2 orders of magnitude. However, the chemical treatment of sulfonation

National Creative Research Center for Block Copolymer Self-Assembly, Department of Chemical Engineering and Polymer Research Institute, Pohang University of Science and Technology, Kyunbuk, 790-784, Korea. E-mail: jkkim@postech.ac.kr

was definitely necessary to make the above-mentioned nanocomposite. Moreover, the percolation threshold was not exactly determined, even though the estimated value was less than 5 wt% of Ppy.

In this study, polystyrene-*block*-poly(*n*-butyl methacrylate) copolymer (PS-*b*-PnBMA) having lamellar microdomains was chosen as a template for the *in situ* polymerization of pyrrole monomer. The rationale for choosing PS-*b*-PnBMA was that py diffuses into only PnBMA microdomain, since py cannot penetrate into PS. Once PS-PnBMA film is immersed into aqueous pyrrole solution and ferric chloride solution sequentially, *in situ* polymerization of pyrrole monomer occurs within the PnBMA microdomains. Also, the diffusion of py into PnBMA microdomains was easily achieved compared with other block copolymers containing SPS or P2VP. This is because the glass transition temperature of PnBMA was ~ 40 °C, lower than those (~ 100 °C) of SPS or P2VP. We found that the amount of Ppy in the PS-PnBMA template was easily controlled by changing the concentration of pyrrole in the aqueous solution and the immersion time. The percolation threshold for these nanocomposites was very low (~ 2 wt% of Ppy).

Experimental

PS-*b*-PnBMA (SBM72) was prepared by sequential addition of styrene and *n*-butyl methacrylate monomers at -78 °C in tetrahydrofuran under argon environment by using *s*-BuLi as an initiator.¹⁸ The molecular weight of PS block was measured by size exclusion chromatography with multi-angle laser light scattering, and the weight fraction of PS block in SBM72 was determined by ¹H NMR spectroscopy. The total weight-average molecular weight (M_w) and polydispersity of SBM72 are 72000 and 1.03, respectively, and the weight fraction of PS block is 0.5. We also used homopolymers of PS and PnBMA prepared by anionic polymerization. The M_w and polydispersity of PS homopolymer are 20600 and 1.03, and those for PnBMA homopolymer are 24500 and 1.05, respectively.

Pyrrole monomer (py) and ferric chloride (FeCl₃) were purchased from Sigma Chemical Co. FeCl₃ acts as both a dopant and an initiator of py. A film of SBM72 with a thickness of 0.3 mm was prepared by compression-molding at 130 °C, and then annealed at 180 °C for 2 days, followed by quenching to room temperature. The film was immersed into a 0.5 M aqueous solution of py for various times at room temperature. Then, it was washed with distilled water until py was completely removed from the film surface. Subsequently, it was immersed into a 1.0 M aqueous FeCl₃ solution for 24 h and washed again with distilled water to remove remaining FeCl₃. After the polymerization of py, the film was dried at room temperature under vacuum for 2 days. The film exhibited a dark color, characteristic of Ppy. The amount of *in situ* polymerized Ppy within the block copolymer matrix was measured by the change of weight before and after the polymerization.

The disorder-to-order transition (LDOT) of SBM72 was measured by SAXS and by rheology. Synchrotron small-angle X-ray scattering measurements were conducted on Beamlines 4C1 and 4C2 at the Pohang Light Source (Korea) where the

W/B4C double multilayer monochromator delivered monochromatic X-rays with a wavelength (λ) of 0.1608 nm and a resolution $\Delta\lambda/\lambda \cong 0.01$ onto the sample.¹⁸ A flat Au mirror was used to reject the higher harmonics from the beam. A 2D CCD camera (Princeton Instruments Inc., SCX-TE/CCD-1242) was used to collect the scattered X-rays. The sample-to-detector distance was 2 m. Samples were exposed for 2 min. A temperature sweep experiment of dynamic storage and loss moduli (G' and G'') was performed under isochronal conditions during heating at a rate of 0.5 °C min⁻¹ by an Advanced Rheometrics Expansion System with parallel plates of 25 mm diameter. The strain amplitude (γ_0) and the angular frequency (ω) were 0.05 and 0.1 rad s⁻¹, respectively, which indicates linear viscoelasticity.

The microdomain structures of SBM72 and nanocomposites with various contents of Ppy were investigated by transmission electron microscopy (TEM; JEOL 1200EX) operating at 120 kV. After a specimen was annealed at 180 °C for 3 days, it was quenched to room temperature. As described below, SBM72 exhibited lamellar microdomains at 180 °C. Cryogenic ultra-sectioning was performed with an RMC (MT-700) microtome with a diamond knife at -100 °C. The Ppy in the nanocomposites was also confirmed by field emission scanning electron microscopy (FE-SEM, Philips) equipped with Energy Dispersive X-ray Microanalysis (EDAX: Model NEW XL-30 132-10) and sapphire detectors.

To confirm whether Ppy was indeed polymerized, the Ppy in a nanocomposite was first extracted by using tetrahydrofuran (THF), since the PS-PnBMA matrix was completely dissolved into THF. Then, the UV spectrum of this solution was obtained with UV spectroscopy (Varian, Cary-5000).

Parallel and perpendicular conductivity measurements were performed on thin films with 300 μ m thickness. Additionally, parallel conductivity was measured using the co-linear four-point probe method. The film surface was covered with silver paste to reduce contact resistance during the measurement. The parallel conductivity (σ_{\parallel}) of the nanocomposites was measured by the four-point probe method with the distance between the electrodes of 1 mm. The sample size was 1×1 cm². The perpendicular conductivity (σ_{\perp}) of the nanocomposites was measured by the two-point probe method. Two electrodes were placed on the top and bottom surfaces of the film.

Results and discussion

Fig. 1 gives temporal changes of G' and G'' for SBM72 upon heating at a rate of 0.5 °C min⁻¹. With increasing temperature, G' decreased gradually and then increased dramatically at 160 °C. This behavior is characteristic of a block copolymer with LDOT, namely, microdomains exist only at higher temperatures.^{19–22} The precipitous increase in G' is referred to as T_{LDOT} .

Fig. 2a gives the changes of the Ppy amounts in the SBM72, PS and PnBMA homopolymers with the immersion time. It is noted that the amount of Ppy in the nanocomposites was measured by the weight change before and after Ppy polymerization in the presence of polymers. It is seen that the amount of Ppy in the PS homopolymer film with a thickness of

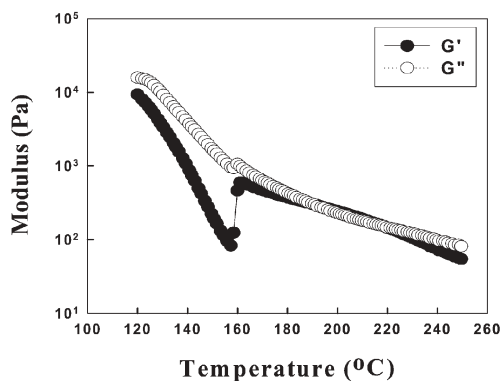


Fig. 1 Temperature dependence of G' and G'' for SBM72.

0.3 mm was negligible even at an immersion time of 5 h. Also, at a given immersion time the amount of Ppy for the PnBMA homopolymer with a thickness of 0.3 mm was about twice that for the SBM72 with the same thickness. These results indicate that py was selectively partitioned into PnBMA microdomains in SBM72. Fig. 2b shows the plots of the amount of Ppy vs. $t^{1/2}$, which indicate that the Fickian law is valid for the PnBMA homopolymer and SBM72. Thus, pyrrole monomers were only diffused into PnBMA lamellar microdomains. The preferential partition of py into PnBMA compared with PS was also investigated by Huijjs *et al.*²³

The doping state of polypyrrole on the SBM72 film surface depending on the immersion times was determined by EDAX analysis, the results of which are given in Fig. 3. Since FeCl_3 was used as both a dopant and an initiator of py, a Cl^- peak should appear due to the counter-ion for the protonated Ppy. The intensity of the Cl^- peak occurring near 2.60 KeV increased steadily with increasing the amount of Ppy.

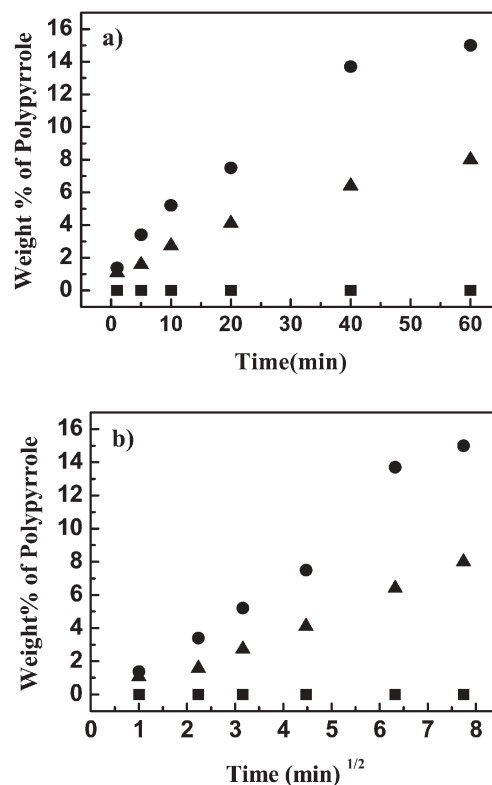


Fig. 2 (a) Plots of weight increase of Ppy (wt%) vs. immersion time. (b) Plots of weight increase of Ppy (wt%) vs. $t^{1/2}$. \blacktriangle : SBM72; \blacksquare : homo PS; and \bullet : homo PnBMA.

However, no peak related to iron was observed, suggesting that all excess FeCl_3 was completely removed during the washing procedure. We found that the concentration of

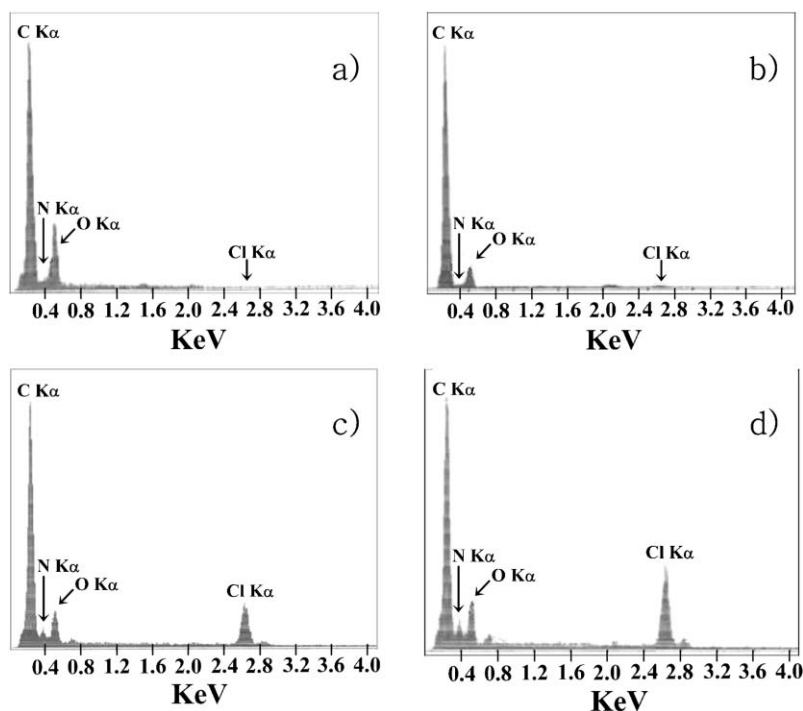


Fig. 3 EDAX results for nanocomposites with various amounts of Ppy. (a) 0.3 wt%; (b) 1 wt%; (c) 3 wt%; and (d) 4 wt%.

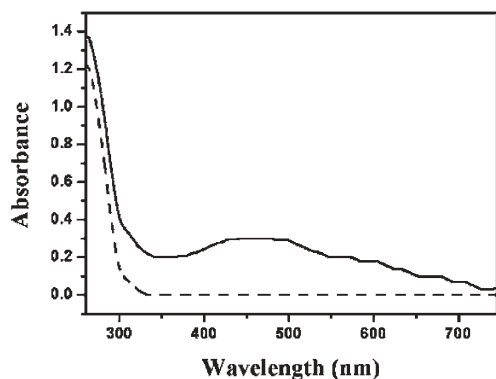


Fig. 4 UV spectra of neat PS-PnBMA (dashed line) and a nanocomposite with 3 wt% of Ppy (solid line).

pyrrole solution was essentially constant (0.5 M) even though the wt% of Ppy was as large as 14 wt%, because the amount of the solution (500 cm³) is much larger than the sample volume (0.068 cm³) of PS-PnBMA film.

Fig. 4 shows the UV spectra of PS-PnBMA and a nanocomposite with 3 wt% of Ppy. A characteristic peak of Ppy, occurring at a wavelength of 452 nm, is clearly observed, indicating that Ppy was indeed synthesized.

Fig. 5a shows a TEM image of SBM72 annealed at 180 °C for 3 days followed by quenching to room temperature. SBM72 exhibited lamellar microdomains with a long spacing (D) of 25 nm. It is noted that dark regions represent PnBMA

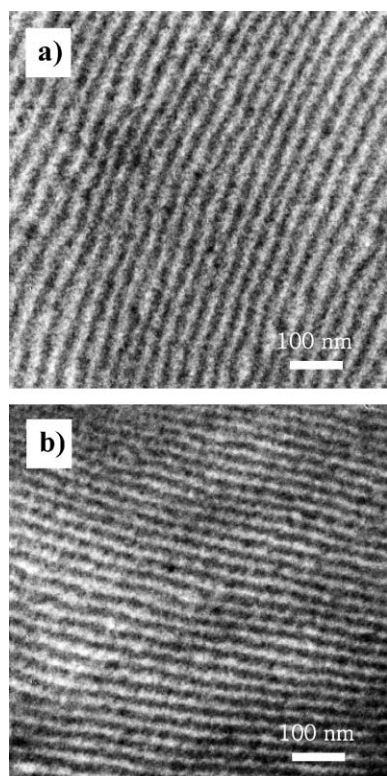


Fig. 5 TEM images for (a) neat SBM72 and (b) a nanocomposite with 14 wt% of Ppy.

microdomains instead of PS microdomains because no staining agent was used. Fig. 5b shows a TEM image of SBM72 with 14 wt% of Ppy, from which lamellar microstructures were clearly observed even for a nanocomposite with 14 wt% of Ppy. However, the exact location of Ppy could not be determined from the TEM image, although Ppy should be located inside the PnBMA microdomains. This is because both Ppy and PBMA block look dark in the TEM image when no staining agent was used.

Maintenance of lamellae even at higher amounts of Ppy suggests that the PBMA lamellar microdomains could play a role as an efficient electrical path in nanocomposites after *in situ* polymerization of pyrrole was done in the block copolymer template. It is also seen from Fig. 5 that D of a nanocomposite with 14 wt% of Ppy is slightly larger than that of neat SBM72 due to the presence of Ppy in PnBMA microdomains.

SAXS profiles ($I(q)$ vs. q ($= 4\pi \sin\theta/\lambda$, where q is the scattering vector and 2θ is the scattering angle) of neat SBM72 and nanocomposites with various amounts of Ppy are given in Fig. 6. Because the electron density difference between PS and PnBMA is very small, higher order peaks except the first order peak were not clearly observed in the SAXS profile. From $D = 2\pi/q^*$, in which q^* is the scattering angle corresponding to the maximum SAXS intensity, D of a nanocomposite with 14 wt% of Ppy was 26.4 nm, which is a small increase (1.3 nm) compared with that for neat SBM72. This is consistent with the TEM images given in Fig. 5. The small increase in D even for a rather large amount of Ppy (14 wt%) can be explained as follows. If 14 wt% of Ppy is assumed to be equally distributed over the entire PnBMA microdomains in the PS-PnBMA film, each lamellar layer of PnBMA contains only ~ 1 wt% of Ppy, since the total lamellar layers of PnBMA in the film with a thickness of 0.3 mm is ~ 1200 layers. Consequently, TEM and SAXS results revealed that the polypyrrole was selectively polymerized inside the PnBMA domain. The increase of D of the nanocomposites with Ppy might be due to the existence of Ppy in PnBMA lamellar domains.

Fig. 7 gives parallel and perpendicular conductivities of nanocomposites with various amounts of Ppy. With increasing the amount of Ppy, these two conductivities did not increase at small amounts of Ppy, then increased dramatically at ~ 2 wt% of Ppy, and finally reached saturated values ($\sim 10^{-1}$ and $\sim 10^{-3}$ S cm⁻¹ for parallel and perpendicular conductivities,

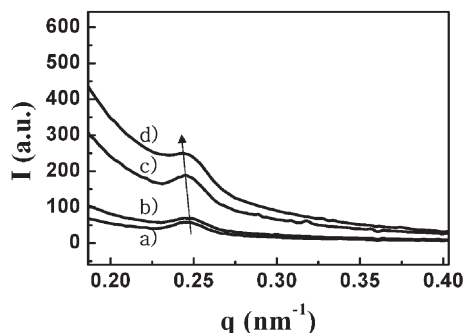


Fig. 6 SAXS profiles for nanocomposites with various amounts of Ppy. (a) 4 wt%; (b) 6 wt%; (c) 8 wt%; and (d) 14 wt%.

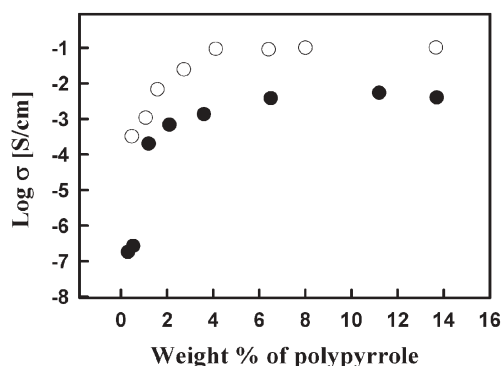


Fig. 7 Parallel (○) and perpendicular (●) conductivities of nano-composites with various amounts of Ppy.

respectively). This indicates that PS-*b*-PnBMA can be used as an effective template for providing effectively electrical paths. It is noted that the saturated value of σ_{\parallel} is about two orders of magnitude higher than that of σ_{\perp} . The main reason for this anisotropic conductance might be due to the orientation of lamellae of SBM72 during the sample preparation. Since the PS-*b*-PnBMA film with a thickness of 0.3 mm was prepared by compression molding and annealed at higher temperature, the parallel orientation of lamellar microdomains to the film surface would be more favored over the perpendicular orientation.

To check the lamellar orientation, we carried out 2D SAXS experiments for neat SBM72 film by irradiating an X-ray beam along the q_y direction (perpendicular to the film surface, as shown in Fig. 8a) as well as the q_z direction (parallel to the film surface). Fig. 8b and c give 2D SAXS patterns in q_x - q_z and q_x - q_y planes, respectively. It is seen that the SAXS

intensity at q^* in the former was more or less uniform along the azimuthal angle, whereas that in the latter exhibited two spots in the meridian and additional second order peaks induced by well-oriented lamellar. Fig. 8d shows the azimuthal plot at q^* for two different planes. It is seen that the parallel orientation of lamellar microdomains in the SBM72 film to the film surface is more favored over the random (or perpendicular) orientation. To determine quantitatively the degree of the orientation of lamellar with respect to the film surface, the orientation factors (f) was evaluated.²⁴

$$f = [3\langle \cos^2\theta \rangle - 1]/2 \quad (1)$$

$$\langle \cos^2\theta \rangle = \frac{\int_0^{\pi} I(q, \theta) \cos^2\theta \sin\theta d\theta}{\int_0^{\pi} I(q, \theta) \sin\theta d\theta} \quad (2)$$

in which θ is the angle of the lamellar normal with respect to the reference direction (q_y). We obtained the values (0.013 and 0.085) of f from Fig. 8b and c, respectively. The different lamellar orientation is the origin of the anisotropy of electrical conductivity.

It is noted that the lamellar orientation can be changed by the sample preparation method. For instance, when a polymer film is prepared by solution casting, a random orientation of lamellae would be expected. On the other hand, when a large amplitude oscillatory shearing is applied to the film, almost perfect alignment of lamellae toward the flow direction can be obtained.²⁵ With increasing the degree of the lamellar orientation toward the flow direction, the anisotropy in the conductivity would increase. This work is currently under way in our laboratory.

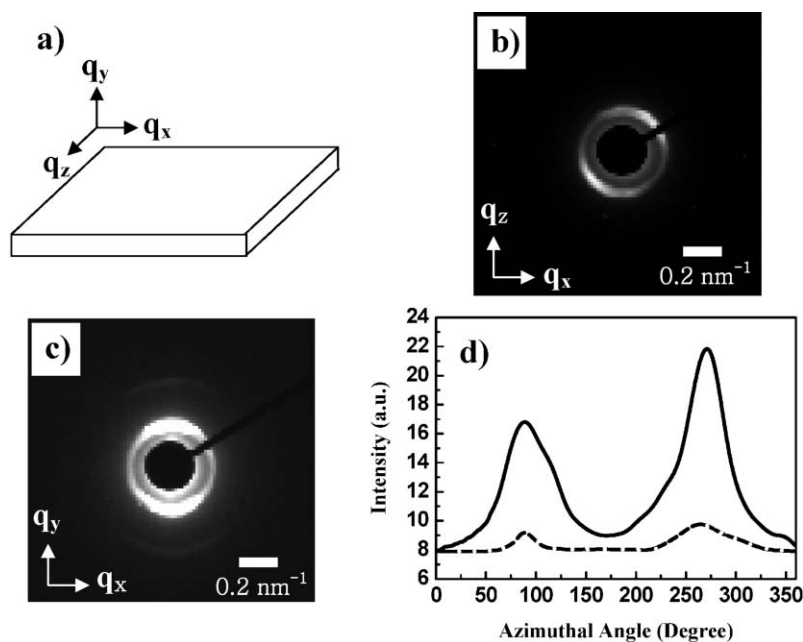


Fig. 8 (a) Schematic of three different directions for 2D SAXS experiments. (b) 2D SAXS image of SBM film irradiated by X-rays along the q_y direction. (c) 2D SAXS image of SBM film irradiated by X-rays along the q_z direction. (d) Azimuthal plots of the intensity at q^* obtained from the q_x - q_z plane (dashed line) and the q_x - q_y plane (solid line). The q_x direction is taken as zero angle.

Conclusion

We have shown that PS-*b*-PnBMA could be used as an effective template for *in situ* polymerization of pyrrole. Since the pyrrole monomer was only partitioned into the PnBMA block, Ppy was only located inside the PnBMA lamellar microdomains. From the measured parallel and perpendicular conductivities of nanocomposites with various contents of Ppy, the percolation threshold concentration of Ppy, above which the nanocomposites behave as semiconductors, was very small (~ 2 wt%). The low value of the percolation threshold was due to the formation of electrical paths resulting from the lamellar microdomains of the PS-*b*-PnBMA. We also showed that the saturated parallel conductivity of the nanocomposites was high ($\sim 10^{-1}$ S cm $^{-1}$), and about two orders of magnitude higher than the perpendicular conductivity. This anisotropy in conductivity results from the preferential orientation of PnBMA lamellar microdomains parallel to the film surface.

Acknowledgements

This work was supported by the National Creative Research Initiative Program by KOSEF. Small angle X-ray scattering (4C1 and 4C2) was performed at PLS beam line supported by POSCO and KOSEF

References

- 1 R. Gangopadhyay and A. De, *Chem. Mater.*, 2000, **12**, 608.
- 2 E. He, M. Omoto, T. Yamamoto and H. Kise, *J. Appl. Polym. Sci.*, 1995, **55**, 283.
- 3 C. Verissimo and O. L. Alves, *J. Mater. Chem.*, 2003, **13**, 1378.
- 4 C. G. Wu and C. Y. Chen, *J. Mater. Chem.*, 1997, **7**, 1409.
- 5 G. Sonmez, P. Schottland, K. Zong and J. R. Reynolds, *J. Mater. Chem.*, 2001, **11**, 289.
- 6 R. I. Stankovic, R. W. Lenz and F. E. Karasz, *Eur. Polym. J.*, 1990, **26**, 359.
- 7 K. Ishizu, Y. Yamada, R. Saito, T. Yamamoto and T. Kanbara, *Polymer*, 1992, **33**, 1816.
- 8 J. Zou, Z. Yu, Y. Pan, X. Fang and Y. Ou, *J. Polym. Sci., Part B: Polym. Phys.*, 2002, **40**, 954.
- 9 T. Wu and S. Lin, *J. Polym. Sci., Part B: Polym. Phys.*, 2006, **44**, 1413.
- 10 W. Thongruang, C. M. Balik and R. J. Spontak, *J. Polym. Sci., Part B: Polym. Phys.*, 2002, **40**, 1013.
- 11 S. Bhattacharyya, S. K. Saha, M. Chakravorty, B. M. Mandal, D. Chakravorty and K. Goswami, *J. Polym. Sci., Part B: Polym. Phys.*, 2001, **39**, 1935.
- 12 M. C. De Jesus, R. A. Weiss and Y. Chen, *J. Polym. Sci., Part B: Polym. Phys.*, 1997, **35**, 347.
- 13 M. C. De Jesus, R. A. Weiss and S. F. Hahn, *Macromolecules*, 1998, **31**, 2230.
- 14 H. L. Wang, L. Toppare and J. E. Fernandez, *Macromolecules*, 1990, **23**, 1053.
- 15 H. L. Wang and J. E. Fernandez, *Macromolecules*, 1992, **25**, 6179.
- 16 R. Mezzenga, J. Ruokolainen, G. H. Fredrickson, E. J. Kramer, D. Moses, A. J. Heeger and O. Ikkala, *Science*, 2003, **299**, 1872.
- 17 I. W. Hamley, *The Physics of Block Copolymers*, Oxford University Press, New York, 1998.
- 18 D. Y. Ryu, U. Jeong, D. H. Lee, J. Kim, H. W. Youn and J. K. Kim, *Macromolecules*, 2003, **36**, 2894.
- 19 T. P. Russell, T. E. Karis, Y. Gallot and A. M. Mayes, *Nature*, 1994, **368**, 729.
- 20 A. V. G. Ruzette, P. Baerjee, A. M. Mayes, M. Pollard, T. P. Russell, R. Jerome, T. Slawacki, R. Hjelm and P. Thiyagarajan, *Macromolecules*, 1998, **31**, 8509.
- 21 R. Weidisch, M. Stamm, D. W. Schubert, M. Arnold, H. Budde and S. Horing, *Macromolecules*, 1999, **32**, 3405.
- 22 U. Jeong, D. Y. Ryu and J. K. Kim, *Macromolecules*, 2003, **36**, 8913.
- 23 F. M. Huijs, F. F. Vercauteren, B. de Ruiter, D. Kalicharan and G. Hadziioannou, *Synth. Met.*, 1999, **102**, 1151.
- 24 L. Wu, T. P. Lodge and F. S. Bates, *J. Rheol.*, 2005, **46**, 1231.
- 25 Z. R. Chen and J. A. Kornfield, *Polymer*, 1998, **39**, 4679.